Available online at www.sciencedirect.com
SCIENCE DIRECT
Cement and Concrete Research 35 (2005) 324–331
CEMENT AND CONCRETE RESEARCH

Effect of carbon fibres on the mechanical properties and corrosion levels of reinforced portland cement mortars

P. Garcés[a,*], J. Fraile[a], E. Vilaplana-Ortego[b], D. Cazorla-Amorós[b], E.G. Alcocel[c], L.G. Andión[a]

[a]Departamento de Ing. de la Construcción, O. Públicas e Infr. Urb. Univ. de Alicante, Apdo. Correos 99. Alicante 03080, Spain
[b]Departamento Química Inorgánica. Univ. de Alicante, Spain
[c]Departamento Construcciones Arquitectónicas, Univ. de Alicante, Spain

Received 29 January 2002; accepted 11 May 2004

Abstract

The changes in mechanical properties of portland cement mortars due to the addition of carbon fibres (CF) to the mix have been studied. Compression and flexural strengths have been determined in relation to the amount of fibres added to the mix, water/binder ratio, curing time and porosity. Additionally, the corrosion level of reinforcing steel bars embedded in portland cement mortars containing CF and silica fume (SF) have also been investigated and reinforcing steel corrosion rates have been determined. As a consequence of the large concentration of oxygen groups in CF surface, a good interaction between the CF and the water of the mortar paste is to be expected. A CF content of 0.5% of cement weight implies an optimum increase in flexural strength and an increase in embedded steel corrosion.

Keywords: Mortars; Carbon fibres; Strength; Corrosion

1. Introduction

As it is well known, carbon fibres (CF) can be obtained from different raw materials, such as polyacrylonitile, rayon, pitches, resins [1] and gases, such as methane and benzene [2]. The first pitch-based CF was prepared in 1963 by Otani and Oya [3]. The pitches used as starting materials for CF preparation are by-products of the coke-making and petrochemical industries. Therefore, these materials have the main advantage of being cheap precursors of CF.

The CF prepared from pitches are mainly classified into two groups according to their properties and precursors [4]: general-purpose CF (GPCF) prepared from isotropic pitches and high-performance CF (HPCF), the latter have excellent tensile strength and modulus and can be prepared from mesophase pitches [4,5].

Fibre composites are new materials based on carbon and other fibre types with exceptional physical and chemical properties suitable to be used in technologically advanced products. Among inorganic fibres, glass fibres are the most widely used nowadays, based on production data. However, the production of CF has shown a fast increment in the last 20 years. This fast growing rate is the result of two factors [6]:

(a) The continuous improvement of these materials' properties.
(b) The cut in production cost, due to improvements of manufacturing process.

There is a wide range of potential applications of GPCF. One of the most important, in terms of the amounts involved, is the use in the construction industry as cement concrete reinforcement.

The CF cement–matrix composites usually contain chopped or milled fibres because continuous fibres present two disadvantages: first, they are more expensive, and second, they cannot simply be added to concrete mixtures. However, it must be noted that chopped or milled CF are mechanically less effective than continuous CF in reinforcing concrete [2].

The surface chemistry of the CF is a very important parameter in order to improve the interaction between the cement matrix and CF. The CF–cement interaction can be modified by different ways, such as thermal treatments [7], or by using chemical agents [8–12].

* Corresponding author.
E-mail address: pedro.garces@ua.es (P. Garcés).

0008-8846/$ – see front matter © 2004 Elsevier Ltd. All rights reserved.
doi:10.1016/j.cemconres.2004.05.013

Although the use of these materials (CF) in construction means an important cost increase, the highly promising benefits of their use, not only because of the improvement of mechanical properties, but also in obtaining more efficient, smaller concrete sections, make it interesting. Based on these advantages and a price reduction, a high growth of demand is expected.

Additionally, due to the good electric conductivity of CF, their addition to concrete produces a very suitable material when that property is important, such as for computer rooms' flooring tiles, which provide a good dissipation of static electricity and avoids electromagnetic interferences in such installations.

Despite the potential advantages of CF, there are very few references in the specialised technical literature about the corrosion behaviour of reinforcing steel embedded in CF portland mortars (CFM) [13]. This paper concludes that "CF decreased the corrosion resistance of rebar in concrete, mainly due to the decrease in the volume electrical resistivity of concrete", which is consistent with the findings of the present paper. However, Ref. [13] only reports of 0.5% CF addition. Bearing in mind the interest of higher rates of CF may be interesting for application, such of electromagnetic shielding, the present paper has gone beyond the experimental conditions of Ref. [13] reporting results for higher CF rates. Therefore, the objective of this paper is to present data about the corrosion kinetics of rebars embedded in CFM with different CF rates.

For that purpose, the behaviour of CFM with different compositions and subject to a broad range of experimental conditions was studied to characterise their durability. The evolution of phases present in the mortars was investigated using XRD spectra. Mortars were also characterised from the point of view of mechanical properties. Compression and flexural strengths were obtained for different CFM compositions, including the addition of silica fume (SF), and curing conditions. Measurements of corrosion rates of reinforcing bars embedded in CFM were carried out along the experiments.

2. Experimental programme

2.1. Materials and specimen preparation

Portland cement type CEM-52.5 (OPC), according to Spanish norms [14], was used. Silica sand with normalised particle size distribution and distilled water were always employed in the mixes. Different values of water/binder ratio (portland cement + SF) were tested, ranging from 0.3 to 0.9. Binder/sand ratio was always 1:3. Commercially available coal tar pitch milled CF provided by Osaka Gas were used for this study (GPCF type). Tables 1 and 2 contain the physical and chemical properties of the milled isotropic-coal tar pitch CF.

Table 1
Physical properties of CF [15]

CF filaments diameter (μm)	13
CF length (mm)	0.13
Tensile strength (MPa)	800
Tensile modulus (GPa)	40
Electrical resistivity (10^{-2} Ω cm)	1
Specific gravity (g cm^{-3})	1.65

Table 2
Chemical properties of CF

O/C surface atomic ratio[a]	0.174
N/C surface atomic ratio[a]	0.014
Carbon content (wt.%)	min. 95

[a] Surface atomic ratio measured by XPS.

The O/C and N/C surface atomic ratios were assessed by X-ray photoelectron spectroscopy (XPS). XPS measurements were carried out with a VG-Microtech Multilab electron spectrometer; the source employed for the measurements was the Mg Kα (1253.6 eV) radiation of twin anode in the constant analyser energy mode. XPS provides information about the chemical composition of the surface of the carbonaceous materials. The O/C ratio indicates the hydrophilic character of the carbonaceous material surface, which can have direct consequences in the fibre–matrix interaction. Then, presumably higher amounts of oxygen groups in the surface of the fibres should improve the fibre–matrix interaction [9].

The CF porous texture have been characterised by gas adsorption (i.e., nitrogen at 77 K and carbon dioxide at 273 K). The adsorption tests were conducted in an Autosorb 6 equipment (see Table 3).

The CO_2 and N_2 volume were calculated by applying the Dubinin–Radushkevich equation. As it can be observed from the Table 3 data, CF present negligible nitrogen adsorption, as corresponds to nonactivated CF, but they contain a small micropore volume detected by CO_2 adsorption, which is related with micropores smaller than 0.7 nm [16].

Content of CF is expressed as percentage of cement mass content. SF was supplied by the Spanish company Ferroatlántica. Mortars were prepared at laboratory ambient conditions (20 °C, 80% RH).

Immediately after casting and surface finishing, moulds were covered with polyethylene films to prevent evaporation of specimen water and then stored. After demoulding (24 h later), specimens were stored in water at laboratory temperature for different curing ages.

Table 3
Characterisation of the porous texture of the CF

Sample	Micropore vol. DR CO_2 (cm^3/g)	Micropore vol. DR N_2 (cm^3/g)	Surface area BET (m^2/g)
Milled CF	0.17	0.01	–

2.2. Testing

The types of specimens and test for the determination of various properties are described below. XRD spectra were obtained to identify the phases present in each case.

2.3. Flexural strength

All specimens, of $4 \times 4 \times 16$ cm size, were tested under laboratory conditions, taken directly from the storage container. Three specimens at each specified age, temperature and w/c ratio were broken by bending with single loading point. The maximum breaking load was determined using a 63-kN capacity miniflexural machine.

2.4. Compressive strength

Six specimens, the specimens sections obtained from the flexural tests, were tested under compression. The crushing load was determined using a 200-kN capacity automatic compression machine. The method used to determine the flexural and compression strengths of mortar prisms was carried out according to Spanish standards [14].

2.5. X-ray diffraction spectra

The XRD experiments were carried out in a Scheifer powder diffractometer with a graphite monochromator and an NaI (Tl) scintillation detector using Cu Kα radiation. The aperture slit of 3° and the detector slit of 0.15° were used. After being crushed in an agate mortar to 40 ì size, the samples were preserved in acetone at 5 °C. The XRD spectra were taken at a speed of $1°\ \mathrm{min}^{-1}$ and the intensities were calculated from the maxima of diffraction after discounting the background.

2.6. Ultrasonic propagation velocity (UPV)

A concrete tester CCT-4 (from CSI) was used for measuring the propagation time of a sonic wave through cement mortar specimens. Two standard cylindrical heads are best suited for such measurements. The measuring surface on the measuring heads must be pressed against the mortar specimens at two exactly opposite points. The surface of the concrete must be reasonably flat and duly cleaned, using vaseline to guarantee good contact. The speed of the ultrasonic sound wave (V in m/s) can be found by the following formula: $V = s \times 10^6/t$ (V: sonic velocity in m/s; s: distance in meters; t: time in microseconds).

2.7. Scanning electron microscope (SEM)

The scanning electron microphotographs were taken with a JEOL JSM-840 SEM equipped with an energy-dispersive X-ray (EDX) and with 20 kV accelerating voltage. High vacuum evaporation (SCD 004 from BALZERS UNION) was the method used for producing a thin gold film to make the specimen surface electrically conductive.

2.8. Porosity (%)

Mortar porosity tests were performed by weighing the specimens in different conditions: dry, saturated in air and saturated while submerged. The percentage taken up by the pores in the specimen volume can be found by the following formula: Porosity $(\%) = (W_{sat} - W_{dry})/(W_{sat} - W_{subm})$ with W_{sat} = weight of the specimens saturated in water (with a vacuum pump); W_{dry} = weight of the specimens dried by heating to 110 °C and later cooled into a chemical desiccator; and Wsubm = weight of the sample in a hydrostatic scale (saturated).

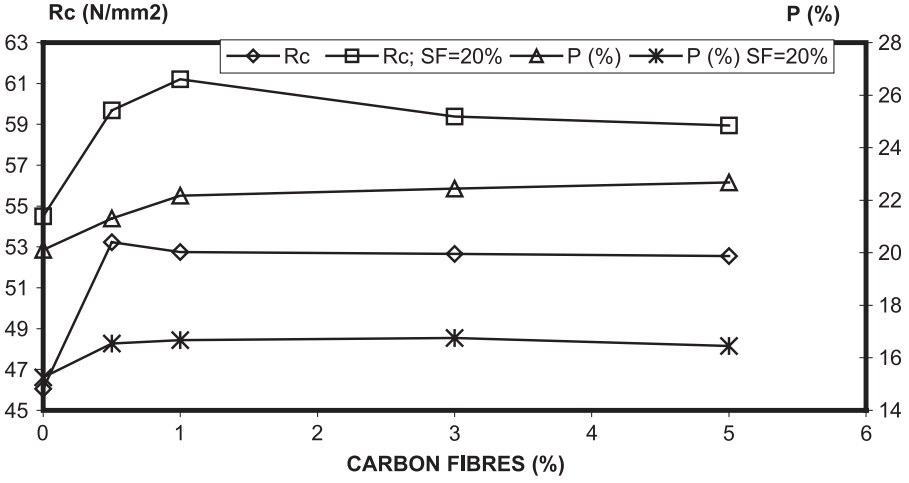

Fig. 1. Relationship between compression strength (Rc, $y1$ axis) and porosity (P, % of specimen volume, $y2$ axis) versus FC content, % of cement mass (x axis), for OPC mortars cured underwater at 20 °C, for 28 days. Influence of 20% of cement mass substitution by SF. Water/binder ratio (cement + SF) = 0.5.

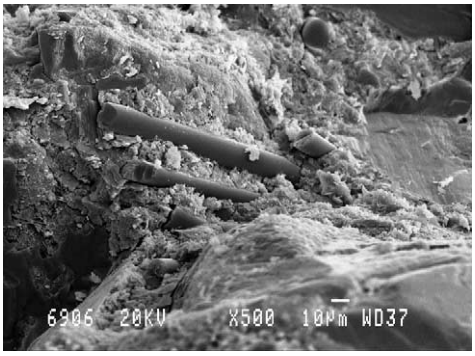

Fig. 2. SEM photo of OPC mortar with 5% addition of CF (curing time: 3 days, 20 °C).

2.9. Corrosion tests specimens

Prisms of 2 × 5.5 × 8 (cm) size were cast, embedding two reinforcing steel and one graphite bar used as electrodes and counterelectrode, respectively, for corrosion tests. After the 28-day curing period, corrosion test specimens were subjected to accelerated carbonation by storing in a chamber holding a CO_2 atmosphere at 20 °C at RH ≅ 58% [17].

2.10. Forced corrosion

Some of the corrosion specimens were subjected to a forced corrosion test by connecting their steel rods to an electrical source providing a constant current density of 20 μA/cm^2 in an initial phase. Then, current density was increased to 30 μA/cm^2 and in a third phase to 50 μA/cm^2. Samples were connected to the power source for as long as required to obtain visible damage in their surface. The total uninterrupted connection time was 600 h.

2.11. Corrosion measurement techniques

The electrochemical technique used to measure the instantaneous corrosion rates was the polarization resistance technique, using the well-known Stern–Geary formula [18,19]. $I_{corr} = B/Rp$. I_{corr} was calculated assuming values of $B = 26$ mV for corroding steel or 52 mV for passive steel. Rp and corrosion potential (E_{corr}) were periodically measured during the time of the experiment, and the weight loss was measured, for each electrode, at the end of the test. All potentials are referred to saturated calomel electrode (SCE). Conductivity was measured always at the end of the test, using a GECOR6 instrument from GEOCISA. This technique is based on the IR-drop from a pulse between the sensor counterelectrode and the rebar network.

3. Results and discussion

3.1. Mechanical and porosity properties

Fig. 1 shows the relationship between compression strength (Rc, $y1$ axis) and porosity (P, % of specimen volume, $y2$ axis) versus % of FC (x axis), for OPC mortars cured underwater at 20 °C, at a curing age of 28 days. The influence of substituting part of the portland cement by SF (20% of cement mass) is also shown. For all cases, it can be observed that the CF addition increases the values of compression strength (Rc) of specimens.

Fig. 2 shows the SEM photo of CF embedded in the OPC mortar mass. It can be observed that the mortar wraps completely the fibre surface. As previously stated, the surface oxygen groups on the CF surface improve the wettability between the CF and the mortar, which is an advantage from a preparation point of view.

Using a small percentage of CF addition, such as 0.5%, a considerable increase in strength is achieved (16%) relative to CF-free mortars, as shown in Fig. 1. For higher CF content values, no significant strength increase over the one obtained for 0.5% is observed, likely due to the increase in sample porosity values. Substitution of part of the mix

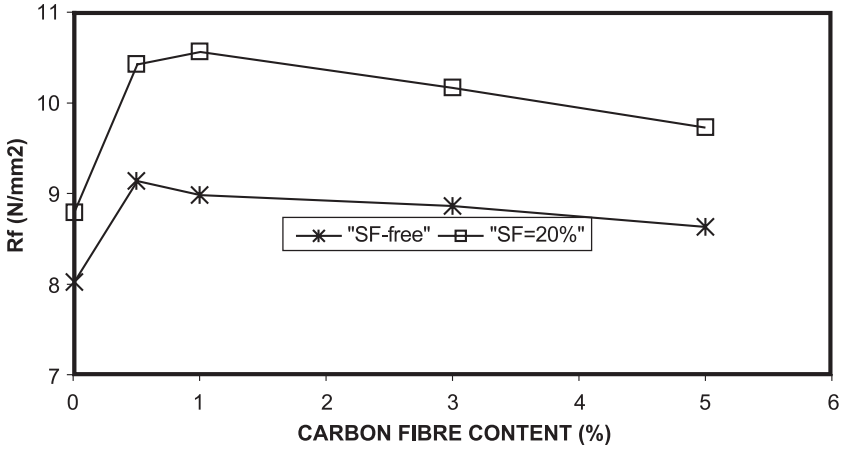

Fig. 3. Relationship between flexure strength (Rf) versus CF content % of cement mass for OPC mortars cured underwater at 20 °C, for 28 days. Influence of substituting 20% of cement mass by SF.

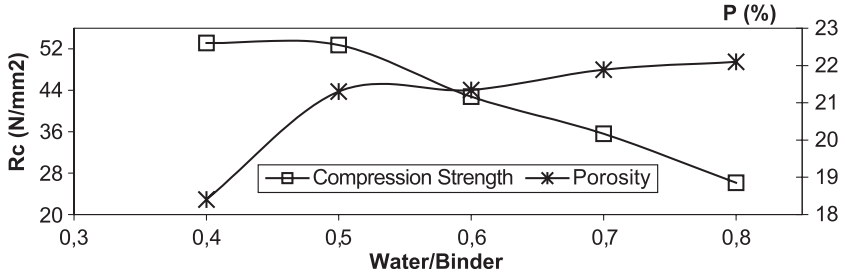

Fig. 4. Relationship between compression strength (Rc, $y1$ axis) and porosity (P, % of specimen volume, $y2$ axis) versus water/binder ratio (x axis) for OPC mortars with 1% of CF respective to cement mass, cured underwater at 20 °C, for 28 days.

cement (20%) by SF also yields to a significant increase in compression strength of the resulting mortar. As can be seen in Fig. 1, increase applies for any amount of CF added, even for CF-free samples, as expected. There is also a significant reduction of specimen porosity for all mixes when SF substitutes part of the portland cement (from 20–22% to 15–16%).

Fig. 3 shows the relationship between flexural strength (Rf) versus CF content for OPC mortars cured underwater at 20 °C, at a curing age of 28 days and with a water/binder ratio of 0.5. With 0.5% of CF, the flexural strength increases about 14% respective to CF-free samples. For amounts higher than 0.5%, the flexural strength gain is either small or negative, probably because the increase of porosity produced by a higher CF content yields to a reduction of mortar strength.

On the one hand, the substitution of OPC by SF increases the flexural strength of samples for any CF percentage as a consequence of the reduction in porosity.

Fig. 4 shows the relationship between compression strength (Rc, $y1$ axis) and porosity (P, $y2$ axis) versus water/binder ratio (x axis), for OPC mortars with 1% of CF, cured underwater at 20 °C, for 28 days. As expected, a steady decrease of compression strength is observed for increasing w/b ratios. Drop reaches 50% between the highest and lowest values.

Fig. 5 shows the relationship of compression strength (Rc, $y1$ axis) and UPV, ($y2$ axis) versus w/b ratios (x axis), for OPC mortar with 1% CF addition cured in water at 20 °C for 28 days. The sound propagation velocity is a function of the mineralogical composition, the intercrystalline connections, the humidity content and, fundamentally, the pore volume of mortar/concrete. In general, when the waves spread in air or water, they suffer a propagation velocity variation. Fig. 4 demonstrates the coherence between these general bases and the results. This similarity in UPV versus w/b curves and compression strength versus w/b curves suggests that it is possible to use this UPV nondestructive test as an empirical determination of compressive strength for mortar with the same proportions of CF/binders/water as those used in the test.

3.2. Corrosion properties

Fig. 6 shows the evolution of the corrosion current density versus time corresponding to steel bars embedded in OPC mortars fabricated with different amounts of CF.

After a 75-day curing period, specimens were hastily carbonated. At the beginning of the test, steel bars of different specimens showed high current density values. Then, I_{corr} reached lower very similar steady values, which is consistent with the low ambient humidity. Thirty days later, the specimens were partially submerged in distilled water. They showed a sudden increase of I_{corr} values different for each of the samples. Sometime later, they reached steady values again. Final values were 0.477, 0.623, 0.64, 0.69 and 0.703 (all μA/cm^2) for samples with CF percentages of 0, 0.5, 1, 3 and 5, respectively.

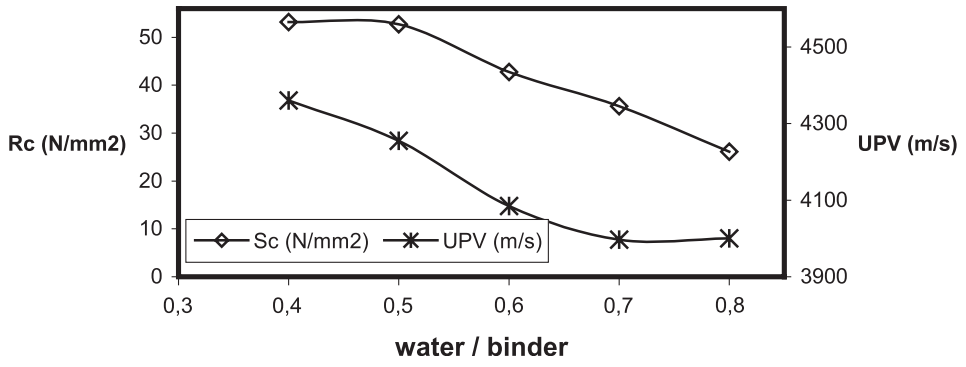

Fig. 5. Relationship of compression strength (Rc, $y1$ axis) and UPV ($y2$ axis) versus w/b ratios (x axis) for OPC mortar with 1% CF addition cured in water at 20 °C for 28 days.

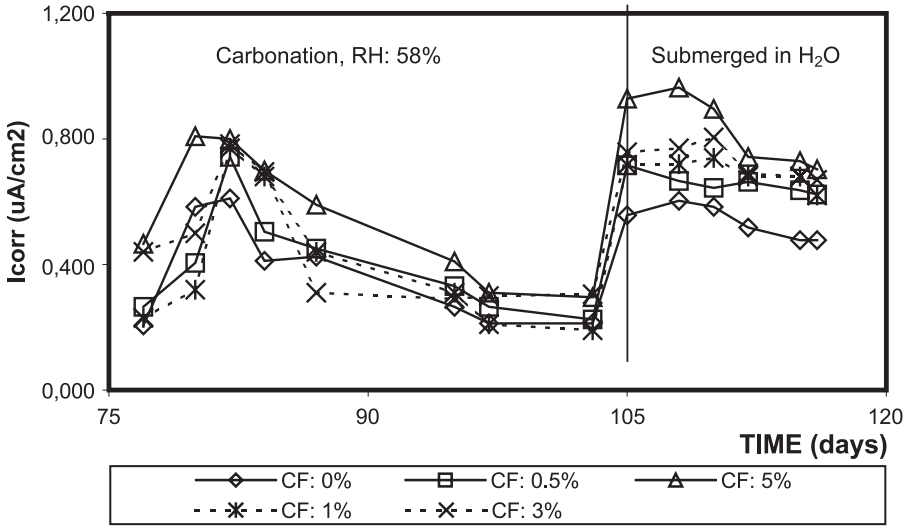

Fig. 6. Evolution of I_{corr} of rebars embedded in OPC mortars with different additions of CF.

Fig. 7 shows the evolution of instant corrosion current density, I_{corr}, with time in mortars with 3% CF, partially submerged in sea water after a 20 °C, HR = 100%, 28-day curing process. Three different mortar formulations are shown: w/b ratios of 0.5 and 0.7 (all portland cement) and w/b = 0.7 and 20% substitution of cement weight by SF. Two facts can be inferred from Fig. 7 observation. First, that corrosion levels increase for higher w/b values, as expected. Second is the remarkable influence of SF addition for improving the corrosion protection of embedded steel in such aggressive environment.

3.3. Checking with the gravimetric losses

The electrochemical loss estimated from the integration of the I_{corr} time curves (Faraday law) has been compared with the corresponding gravimetric losses. Rp measurements versus gravimetric losses are presented in Fig. 8, and it can be observed that all points lie inside the error factor of two reported by Stern (3) for Rp measurements. Therefore, the B values assumed (26 mV) may be considered as correct enough.

3.4. Forced corrosion

The corrosion of steel in reinforced concrete/mortar members produces in a number of years serious consequences in their structural integrity, such as cracking, spalling of concrete cover, steel section reduction and loss of steel–concrete bonding, all of which are critical for the combined structural behaviour of both member materials.

One of the ways utilised by some authors to produce a considerable amount of corrosion products out of the rebars and thus obtain information about the long-term damage in a reasonable experimental time consists in applying a constant anodic current to the bars for a period of time and observe the amount of corrosion that yields to cracking. In this research, part of the specimens with 0.5 and 0.7 w/b

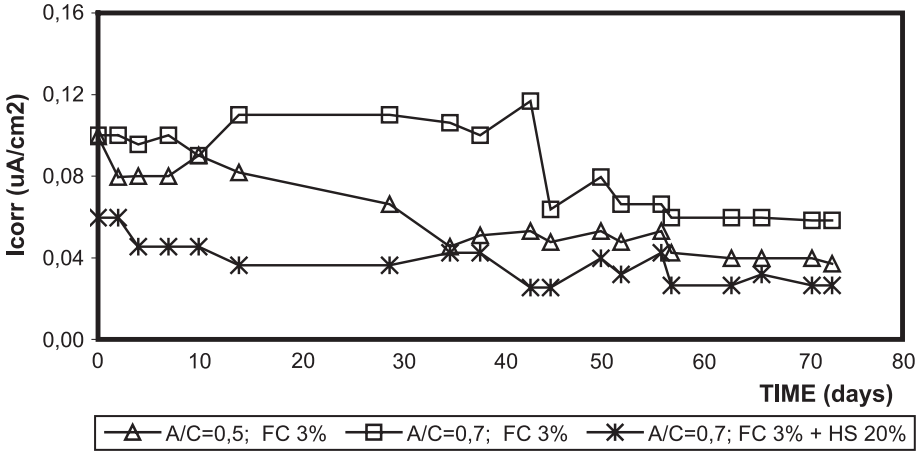

Fig. 7. Evolution of instant current density I_{corr} versus time in OPC mortars fabricated with w/b ratios of 0.5 and 0.7 and 3% content of CF, partially submerged in sea water. Influence of 20% substitution of cement mass by SF.

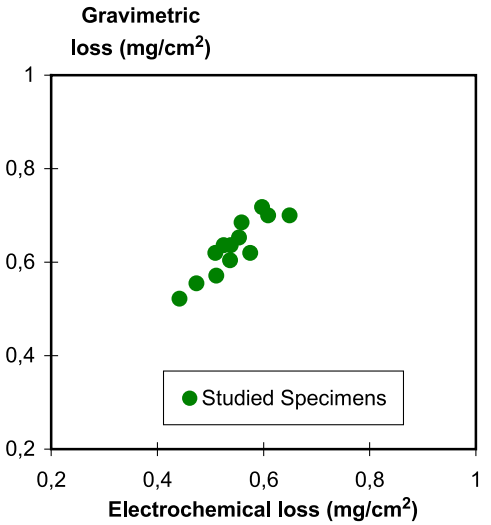

Fig. 8. Comparison between electrochemical and gravimetric losses in mortar specimens studied.

ratios and different CF contents were subjected to forced corrosion.

At the end of forced corrosion tests, samples were demolished to obtain the loss of iron mass due to the corrosion process by direct weighing and compare the results with the theoretical values calculated using Faraday law. Mass loss values were 318 and 333 mg for samples with w/b ratios of 0.5 and 0.7, respectively (without SF). In samples with 20% substitution of cement by SF and w/b = 0.7, the mass loss was smaller than in the other two (only 311 mg), as expected, based on the observations of damage along the corrosion process, confirming again that this substitution reduces the effects of steel corrosion in mortars.

3.5. XRD tests

Samples of each of the above described specimens were tested by XRD. In all cases, the only phases encountered were the typical ones found in portland cement mortars. This confirms that no chemical reaction between CF and hydrated phases of cement has occurred.

4. Conclusions

(1) As a consequence of the large concentration of oxygen groups in CF surface, a good interaction between the CF and the water of the mortar paste is to be expected.
(2) An optimum increase in flexural strength is obtained for a CF content of 0.5% of cement weight in the mortar. The substitution of OPC by SF increases the flexural strength of samples for any CF percentage as a consequence of the reduction of porosity.
(3) The great similarity in UPV versus w/b curves and compression strength versus w/b curves suggests that it is possible to use this UPV nondestructive test as an empirical determination of compressive strength for mortar with the same proportions of CF/binders/water as those used in the test.
(4) The addition of CF increases corrosion current density I_{corr} in embedded steel, probably due to the drop of electrical resistivity [20]. The higher the CF, the higher are the I_{corr} values in rebars.
(5) Mortars prepared with CF addition and substitution of 20% of portland cement weight by SF have a notable reduction of porosity and instant corrosion rate of embedded reinforcement.

Acknowledgements

The authors would like to acknowledge financial support received from the Generalitat Valenciana (Spain; CTIDIB/2002/164), from Ministerio de Ciencia y Tecnologia (MAT 2003-06863) and from Ministerio de Fomento.

References

[1] The Economics of Carbon Fibre, 2nd ed., Roskill Information Services, 2 Clapham Road, London SW9 OJA, 1990.
[2] A. Madroñero, Possibilities for the vapour–liquid–solid model in the vapour-grown carbon fibre growth process, J. Mater. Sci. 30 (1995) 2061.
[3] S. Otani, A. Oya, Progress of pitch-based carbon fiber in Japan, in: J.D. Bacha, J.W. Newman, J.L. White (Eds.), Petroleum-Derived Carbons, ACS Symposium Series, vol. 303, 1986, pp. 323–334.
[4] T. Maeda, S.M. Zeng, K. Tokumitsu, J. Mondori, I. Mochida, Preparation of isotropic pitch precursors for general purpose carbon fibres by air blowing: I. Preparation of spinnable isotropic pitch precursor from coal tar by air blowing, Carbon 31 (3) (1993) 407.
[5] J.B. Donnet (Ed.), Carbon Fibres, Marcel Dekker, New York, 1998, pp. 311–369.
[6] D.D.L. Chung, Cement reinforced with short carbon fibers: a multifunctional material, Composites: Part B. Engineering 31 (6–7) (2000) 511–526.
[7] T. Sugama, L.E. Kukacka, N. Carciello, D. Stathopoulos, Interfacial reactions between oxidized carbon fibers and cements, Cem. Concr. Res. 19 (3) (1989) 355–365.
[8] X. Fu, W. Lu, D.L.L. Chung, Improving the bond strength between carbon fiber and cement by fiber surface treatment and polymer addition to cement, Cem. Concr. Res. 26 (7) (1996) 1007–1012.
[9] X. Fu, W. Lu, D.L.L. Chung, Ozone treatment of carbon fiber for reinforcing cement, Carbon 36 (9) (1998) 1337–1345.
[10] Y. Xu, D.L.L. Chung, Carbon fiber reinforced cement improved by using silane-treated carbon fibers, Cem. Concr. Res. 29 (5) (1999) 773–776.
[11] T. Yamada, K. Yamada, R. Hayashi, T. Herai, International SAMPE Symposium and Exhibition, vol. 36, SAMPE, Covina, CA, 1991, pp. 362–371, Pt 1.
[12] T. Sugama, L.E. Kukacka, N. Carciello, B. Galen, Oxidation of carbon fiber surfaces for improvement in fiber–cement interfacial bond at hydrothermal temperature of 300 °C, Cem. Concr. Res. 18 (2) (1988) 290–300.
[13] J. Hou, D.D.L. Chung, Effect of admixture in concrete on the corrosion resistance of steel reinforced concrete, Corros. Sci. 42 (2000) 1489–1507.

[14] UNE-EN 197-1:2000: "Cemento. Parte 1: Composición, especificaciones y criterios de conformidad de los cementos comunes.
[15] Renoves L Series. Application of Donacarbo-S, Osaka Gas, Product catalogue.
[16] D. Cazorla-Amorós, J. Alcañiz-Monge, M.A. De la Casa-Lillo, A. Linares-Solano, CO_2 as an adsorptive to characterise carbon molecular sieves and activated carbons, Langmuir 14 (16) (1998) 4589–4596.
[17] ASTM, E-104-71: Maintaining constant relative humidity by means of aqueous solutions, 1988.
[18] M. Stern, A.L. Geary, A theorical analysis of the shape of polarization curves, J. Electrochem. Soc. 104 (1) (1954) 56.
[19] C. Andrade, J.A. Gonzalez, Techniques electrochimiques qualitatives et quantitatives pour mésurer les effects des additions sur la corrosion des armatures, Silic. Ind. 47 (1982) 289–295.
[20] C. Pu-Woei, D.D.L. Chung, J. Electr. Mater. 24 (1995) 47–51.